

Journal of Climate Change, Vol. 2, No. 1 (2016), pp. 53–60. DOI 10.3233/JCC-160006

Spring "Predictability Barrier" and Indian Summer Monsoon

A.P. Dimri

School of Environmental Sciences, Jawaharlal Nehru University, New Delhi, India

apdimri@hotmail.com

Received December 4, 2015; revised and accepted December 30, 2015

Abstract: Monthly correlation of Indian monsoon rainfall (IMR) index with various monsoon indices changes predominantly and peaks within summer season (Ailikun and Yasunari, 2001). There is transition in this lead and lagged correlation during spring (March, April and May). This spring transition could not be captured in many general circulation models (GCMs) and is termed as "predictability barrier" (Latif and Graham, 1991). It has been less investigated and hence reasons for dampening/reversal of associated large scale fields during spring are intriguing.

Present study illustrates dynamics of spring predictability barrier with Indian summer (June, July, August and September) monsoon (ISM). In this study, based on data from 1979 to 2008, an internal dynamics between various monsoon indices and corresponding IMR anomaly is diagnosed. It is found that secular behaviour of El Niño–Southern Oscillation (ENSO) during preceding spring of monsoon months (June, July, August and September) gets reversed in succeeding spring. Though correlation between various monsoon indices and ISM index remains similar during preceding and succeeding springs with peaks during monsoon (June, July, August and September), corresponding large scale fields show that strong significant convection dominates over the southern equatorial eastern Pacific Ocean, northern equatorial western Pacific Ocean, Indonesian throughflow and weaker significant convection dominates over the Head Bay of Arabian Sea and western to central Indian sub-continent during preceding spring. Such patterns reverse during succeeding spring.

Keywords: Spring predictability barrier; Indian summer monsoon; Correlation.

Introduction

Indian summer monsoon (ISM) has socio-economic importance for the Indian sub-continent. Most of the agricultural based economy of India is very much dependent on it. Many facets of it are studied by various researchers (Annamalai et al., 2007; Krishnakumar et al., 1999, 2006; Turner et al., 2011). The El Niño—Southern Oscillation (ENSO) is an important air—sea coupled system (Yasunari, 1990) that plays a dominant role in defining variability over different regions of the world at various spatio-temporal scales. In the last decade, changes in El Niño patterns have been reported by many studies (Yeh et al., 2009; Kim et al., 2009;

Karamuri et al., 2007, 2009). A declining relationship of ENSO with the Indian summer monsoon (ISM) has been observed by various researchers (Kriplani and Kulkarni, 1997; Krishnakumar et al., 1999, 2006; Kuchraski et al., 2007; Saha et al., 2012). Many of these studies have used Indian monsoon rainfall (IMR) index to represent intensity of ISM. This index is calculated based on the land-based rain gauge observed data (Sontakke et al., 1993; Parthsarthy et al., 1995) and proved very useful for evaluating ISM.

Relationship between ISM and ENSO, its interannual variability, the persistence of ISM/ENSO in the seasonal cycle remains an important issue. But a very few researchers and studies have shown the critical threshold

on understanding such relation during spring (March, April and May). Latif and Graham (1991) illustrated limitation in prediction in global climate models (GCMs) during this period which is called spring predictability barrier. During this time—spring predictability barrier drop off of persistence in central Pacific precipitation, eastern pacific sea surface temperature (SST), southern oscillation index (SOI) and other ENSO indices are seen (Wright, 1979, 1985). Torrence and Webster (1998) gave a plausible reasoning of phase locking of ENSO to the annual cycle, which cause the spring predictability barrier. Still, the anomalous state of ENSO-monsoon system likely persists through the spring predictability barrier of the ENSO (Webster and Yang, 1992), e.g., the upper tropospheric zonal wind over south Asia is noted to maintain the same anomalous state from the previous winter to the summer monsoon season. Yang et al. (1996) pointed out that the precursory signals of Asian summer monsoon are associated with the anomalous state of tropical SST and convection in the previous winter.

Since not enough dynamical understanding of spring predictability barrier is available, here study is planned to look into the spring predictability barrier with ISM using various monsoon indices defined by various researchers. Webester and Yang (1992), Goswami et al. (1999) and Wang and Fan (1999) defined set of monsoon circulation indices by objectively analyzing wind fields. Webster and Yang (1992) used vertical shear of zonal component of wind between lower (850 hPa) and upper (200 hPa) troposphere over southern Asia and Indian Ocean (5°-20°N, 40°-110°E) to define an index, hereafter called WYI. Goswami et al. (1999) suggested contribution of other processes in defining ISM and defined another index using vertical shear of meridional component of wind between lower (850 hPa) and upper (200 hPa) troposphere over Indian region (10°-30°N, 70°-110°E), hereafter called BNI. Following, Wang and Fan (1999) provided comprehensive overview and discussion on choice of the indices and suggested a new index by defining difference of zonal component of wind at lower (850 hPa) troposphere between averaged over 5°-15°N, 40°-80°E (region 1) and 20°-30°N, 70°-90°E (region 2), hereafter WFI. Corresponding regions are shown in Figure 1.

With such preamble, the present study specifically looks into the spring predictability barrier and its associated ISM during excess and deficit composite years. Behaviour during preceding and successive spring months of monsoon (June, July, August and September)

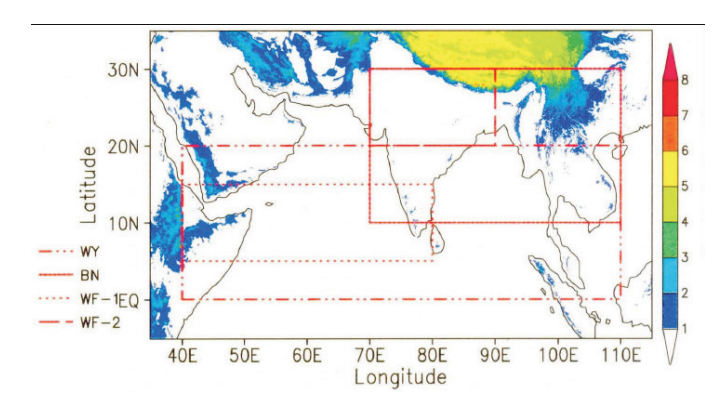
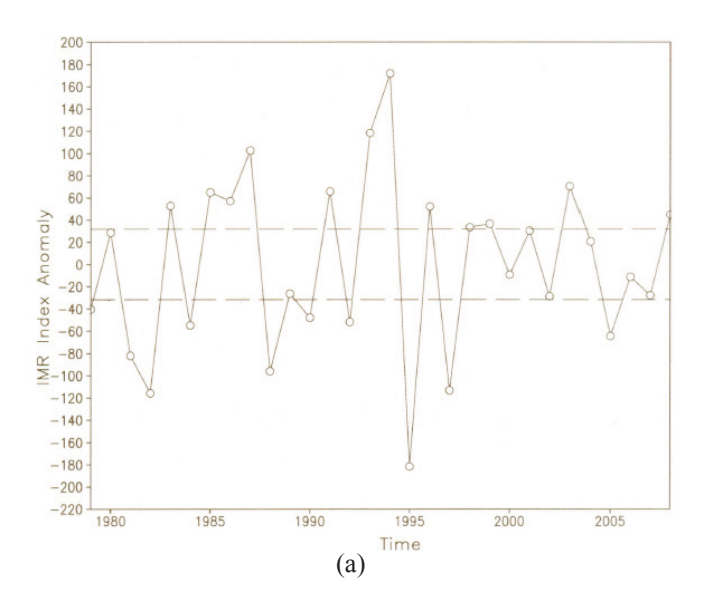


Figure 1: Topographic (m×10³) depiction over Indian subcontinent. Boxes correspond to monsoon indices as defined by Webster and Yang (1992) (5°-20°N, 40°-110°E): WYI; Goswami et al. (1999) (10°-30°N, 70°-110°E): BNI and Wang and Fan (1999) (5°-15°N, 40°-80°E: region 1) and (20°-30°N, 70°-90°E: region 2): WFI – 1 and 2.

is deliberated upon. Above indices are also analyzed in determining this.

Data and Methodology

IMR index anomaly time series is taken from Indian Institute of Tropical Meteorology (IITM), Pune, India to define the excess and deficit precipitation years. These excess and deficit years are considered based on ±1 standard deviation. Based on this 12 years (1983, 1985, 1986, 1987, 1991, 1993, 1994, 1996, 1998, 1999, 2003 and 2008) are found to be excess precipitation years and 10 years (1979, 1981, 1982, 1984, 1988, 1990, 1992, 1995, 1997 and 2005) are found to be deficit precipitation years. Precipitation record from APHRODITE (Yatagai et al., 2012) at 0.25° horizontal resolution is used to assess monsoon (June, July, August and September) precipitation distribution over the Indian subcontinent. It is important to mention here that the number of stations per grid cell is available for APHRODITE. This information could be very useful to determine to what extent the gridded precipitation is determined from station data or derived using interpolations between the stations. Observing multiple meteorological elements could monitor weather changes associated with maturing of large scale circulations (Ueno et al., 2008). In addition, NCEP/NCAR II reanalysis large scale fields at 2.5° horizontal resolution (Kanamitsu et al., 2002) and Hadley centre sea surface temperature (SST) at 1° horizontal resolution (Hadley Centre, 2006) is also used for the study. Also, long term satellite estimates of outgoing longwave radiation (OLR) data provide important information to diagnose variability of climatic conditions during different phases of El Niño. The National Oceanic and Atmospheric Administration (NOAA), US interpolated OLR data (Liebmann and Smith, 1996) is used to identify such seasonal and ground dependency. This data is distributed in 2.5° grid with monthly time interval. Monthly OLR variability is one of the good indicators of cloud formations associated with precipitation.



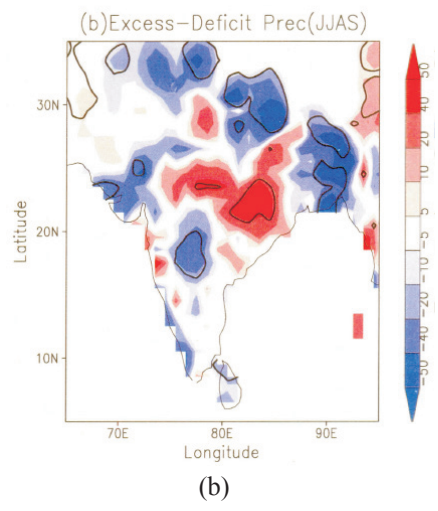


Figure 2: (a) Interannual cycle of IMR index during 1979-2008. There are significant excess (1983, 1985, 1986, 1987, 1991, 1993, 1994, 1996, 1998, 1999, 2003 and 2008) and deficit (1979, 1981, 1982, 1984, 1988, 1990, 1992, 1995, 1997 and 2005) years based on ±1 standard deviation where such peaks dominate and (b) Corresponding difference in ISM precipitation composites during deficit and excess years. Significant deficit (excess) precipitation over the mideast of Indian subcontinent (foothills of the Himalayas) is seen. Another significant excess zone of precipitation is seen over the Indian Deccan Plateau.

Results and Discussion

Firstly, a brief on IMR index and corresponding precipitation difference between composite of excess and deficit years is illustrated in Figure 2. Figure 2a illustrates the interannual cycle of IMR index during 1979-2008. There are significant excess and deficit years where such peaks dominate. Corresponding difference in ISM precipitation composites during deficit and excess years are presented in Figure 2b. Significant deficit (excess) precipitation over the mideast of Indian subcontinent (foothills of the Himalayas) is seen. Another significant excess zone of precipitation is seen over the Indian Deccan Plateau.

As discussed in the introduction, interannual variability of the ISM has different relationship with tropical atmosphere/ocean system of ENSO through analyzing different types of monsoon indices (WYI, BNI and WFI). To exhibit it more clearly, a lead (lag) correlation of each monsoon index in summer (June, July, August and September) with the Nino3.0 SST in preceding (succeeding) months are depicted in Figure 3. Figure illustrates the 21 years sliding correlation of monsoon indices and IMR during summer with the

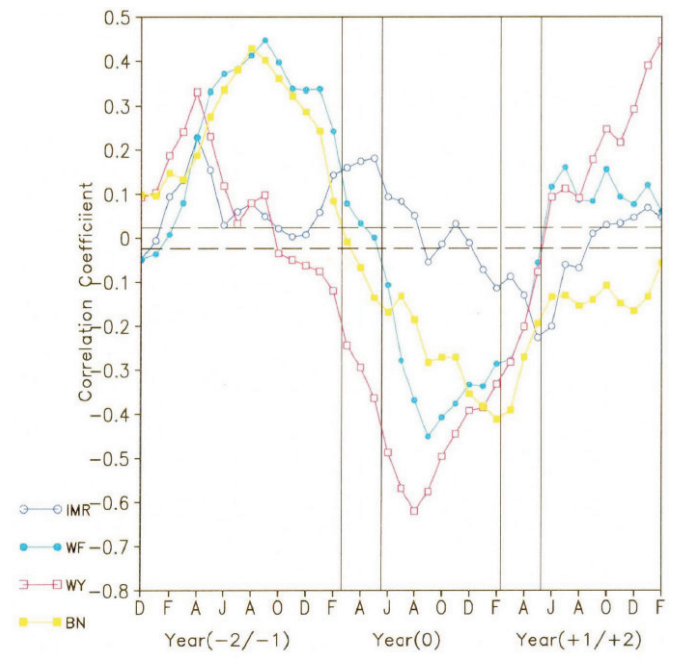


Figure 3: Lead (lag) correlation of monsoon indices and IMR during summer (June, July, August and September) with the Nino3.0 SST during preceding (succeeding) month. During preceding (succeeding) spring (March, April and May) increased (decreased) positive (negative) correlation with IMR is seen, which is opposite to as seen with all the three monsoon indices.

Nino3.0 SST during preceding month. This constructs the basis of lead and/or lag analysis among them. The significant positive correlation among all the indices with the Nino3.0 SST dominates during preceding summer (June-September) and winter (December-February) and succeeding summer (June-September) and winter (December-February). This implies that there is strong vertical and horizontal zonal wind shear and strong vertical meridional wind shear dominated during this period. Concurrent summer seasons show significant negative correlation with all the indices, thus suggesting that these shears weaken or reverse during the concurrent season. It is noticed that WYI shows a kind of lag in correlation with summer precipitation than that in WFI and BNI during preceding seasons which no more exist in succeeding seasons. In addition, Figure 3 shows internal variability of IMR index which has quasi-biennial oscillation with the reversal of correlations between year (-1) and year (0), but other indices don't show that. This is suggested by Ailikun and Yasunari (2001) too. Thus, here it is specifically analyzed what happens during spring predictability barrier?

Interestingly, though, it is observed that during this period correlation of wind indices reverses as compared to preceding and succeeding seasons. IMR index has opposite correlation with other three wind indices during the spring period. During preceding (succeeding) spring correlation of IMR index with Nino3.0 SST reaches to the highest positive (negative). Corresponding wind indices show increased negative (positive) correlation with Nino3.0 SST during preceding (succeeding) spring. Torrence and Webster (1998) explained possible mechanism of annual cycle ENSO's phase locking during spring. It is distinctly seen that, the correlation patterns show a systematic transition during spring. The critical change of the physical processes in the interaction between ENSO and ISM is suggested to occur during spring. Thus, in terms of the interannual variability, spring season plays a crucial role in determining strength of ISM. Thus in the following sections circulation difference in composites of excess minus deficit years' corresponding to ISM is elaborated.

To investigate it further, regional analysis of wind over respective indices' regions is performed. From WFI, two regions are considered separately to assess the wind circulation (hereafter WF-1 and WF-2). Area averaged vertical wind and temperature differences between composites of excess and deficit years over regions WF-1, WF-2, WY and BN are presented in Figures 4a, 4b, 4c and 4d respectively. Figure 4a

corresponds to the region WF-1 and it shows that during pre ISM period lower (1000 hPa – 850 hPa) and higher (400 hPa – 200 hPa) troposphere has stronger westerlies during excess years than that during deficit years. And mid (800 hPa – 400 hPa) and upper (200 hPa and above) troposphere has weaker westerlies during excess years than that during deficit years. This corresponds to the fact that tropical easterly jet at 200 hPa and Somali jet at 850 hPa strengthens before the ISM (Koteswaram, 1958) during excess precipitation years.

In subsequent months of the ISM westerly weakens all across from surface to upper troposphere. Corresponding distribution over WF-2 region shows peculiar vertical wind distribution (Figure 4b). At lower (900 hPa -600 hPa) and upper (300 hPa - 200 hPa) troposphere weaker westerlies, in mid (600 hPa - 400 hPa) and higher (~100 hPa) troposphere stronger westerlies dominate during excess years than that during deficit years of precipitation. Apart from that, there is a kind of cascading increase and decrease in the westerly strength as it marches during the considered period. Such distribution shows surges of increase/decrease in westerly strength over the region as the season advances. Over WY region, Figure 4c, area average vertical wind distribution is very similar to that over the WF-1 region. Over BN region, Figure 4d, southerly wind gradually strengthens with season in the lower (1000 hPa - 700 hPa) and mid (500 hPa - 200 hPa) troposphere with a weakening of southerly winds over lower mid (850 hPa – 500 hPa) troposphere around the ISM monsoon time in excess years than that during deficit precipitation years. Such gradual increase in the lower and mid-upper troposphere corresponds to more southern flux during ISM time.

Corresponding area averaged vertical temperature difference over the WF-1 region (Figure 4a) shows colder temperature in excess year in preceding and succeeding seasons of ISM. But during ISM all across the vertical pressure levels warmer temperatures prevail during excess years than during deficit years. Over WF-2 region, Figure 4b, generally warmer (colder) temperatures prevail during preceding (succeeding) season. However, discernible feature of mid troposphere shows that lower temperature during ISM dominates during excess precipitation years. During excess precipitation years area averaged vertical temperature distribution over the WY region suggests colder (warmer) temperature before (after) ISM season and are very much in accordance with that over the WF-1 region (Figure 4c). In case of BN region, Figure 4d, warmer (colder) temperature prevail before (after) the monsoon

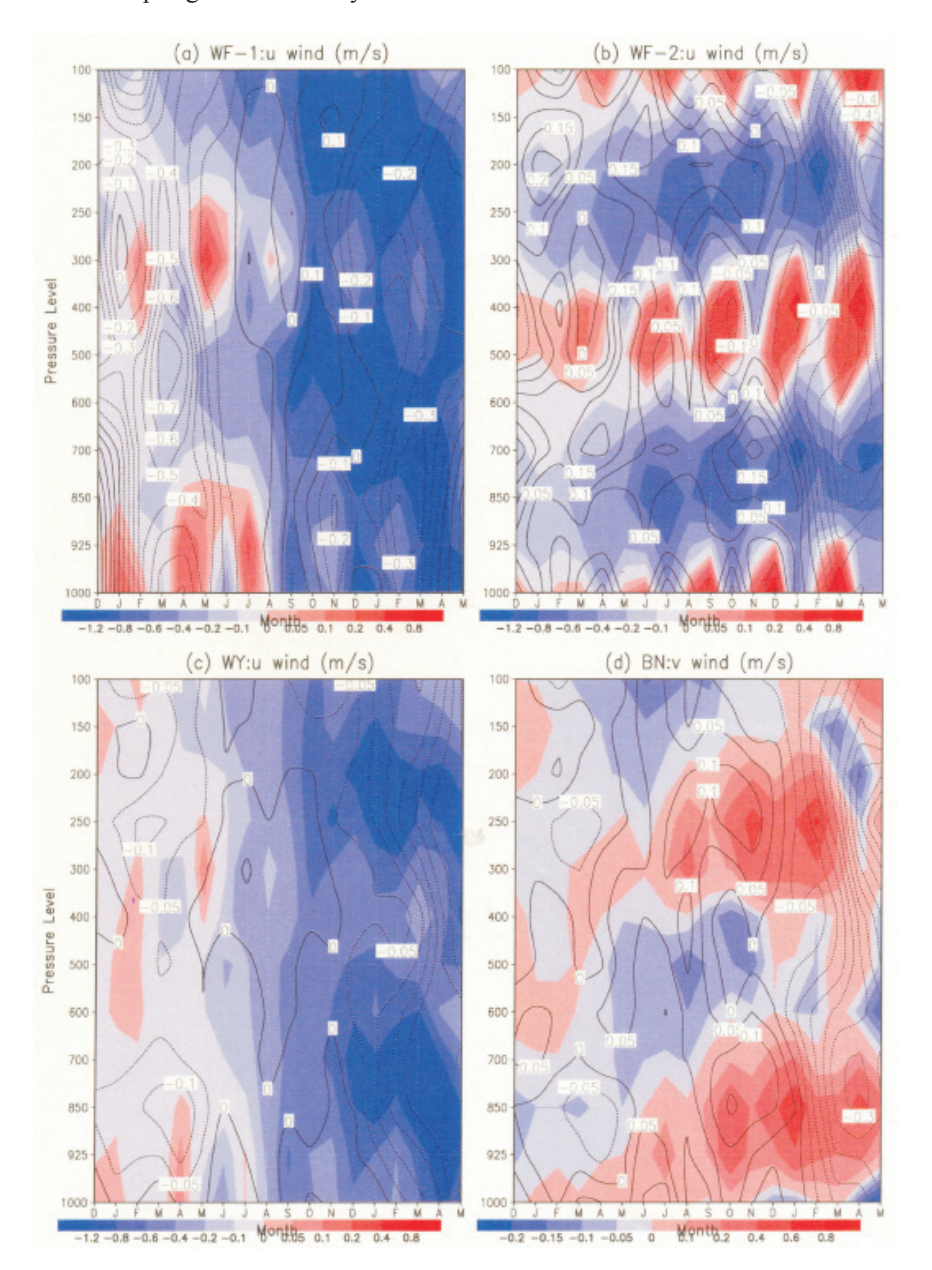


Figure 4: Area averaged zonal wind (shaded: m/s) and temperature (contour: °C) differences between composites of excess and deficit years over regions (a) WF-1, (b) WF-2, (c) WY and (d) BN (here it is meridional wind (m/s) as this indices depends on meridional wind).

season, with a specific cooling in lower (~800 hPa) and upper (~250 hPa) troposphere before the ISM season.

Corresponding role of preceding and succeeding spring SST with the ISM is analyzed and is presented in Figure 5a and 5b respectively. Correlation plots in shade and significant regions at 99% confidence interval are shown. Figures 5a and 5b show very contrasting patterns coupled with spring and ISM. During preceding spring significant colder (warmer) SST over north (south) equatorial Pacific dominates. Also, significant warmer temperature over Indian

Ocean exists. During succeeding spring this patterns get reversed. Almost all equatorial Pacific Ocean shows significant warming, except over eastern equatorial Pacific Ocean adjacent to the southern American coast, where it shows significant colder temperature patterns (Figure 5b). Over Indonesian Indian Ocean too similar significant colder patterns emerge. Further investigation of coupling of ISM with preceding and succeeding spring is illustrated with composite difference of OLR and 850 hPa wind between excess and deficit years in Figures 6a and 6b respectively. During preceding

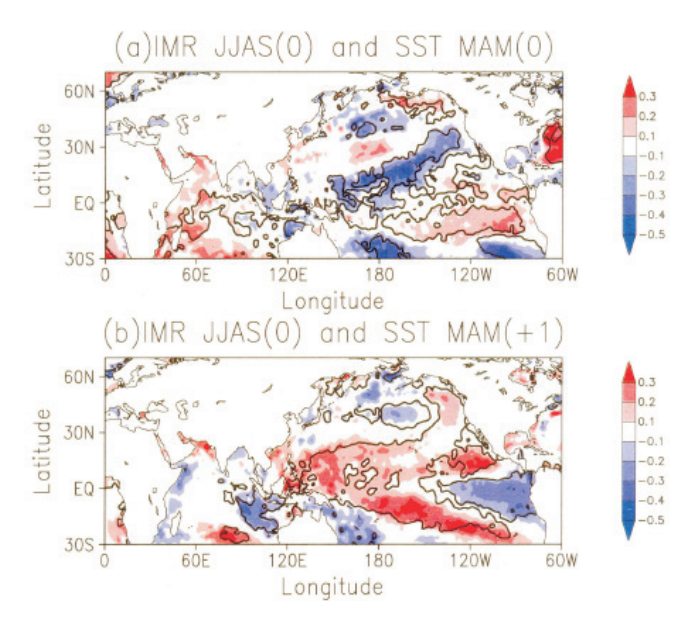


Figure 5: Correlation (shaded) plot between summer (June, July, August and September) monsoon rainfall with SST of (a) preceding spring and (b) succeeding spring respectively. Black contours represent regions (and not the correlation) significant at 99% confidence interval.

spring, Figure 6a, strong significant convection over the southern equatorial eastern Pacific Ocean, northern equatorial western Pacific Ocean and Indonesian throughflow dominates. Weaker significant convection over Head Bay of Arabian Sea and western to central Indian subcontinent dominates, which in succeeding spring, Figure 6b, reverses in a way. Strong convection zone over southern equatorial eastern Pacific Ocean during preceding spring shows weaker convection during succeeding spring. Additionally, strong zones of convection over northern equatorial western Pacific Ocean and central Pacific Ocean along with weaker convection over northern equatorial central Pacific Ocean are discernible. Also, a significant zone of convection over the southern eastern Indian subcontinent is seen. Corresponding 850 hPa winds shows weaker westerlies over the eastern equatorial Pacific Ocean and Indian Ocean during preceding spring (Figure 6a). In addition significant stronger northwesterly over Indian subcontinent prevail. In case of succeeding spring, Figure 6b, strong divergence over eastern equatorial Pacific Ocean is illustrated. Further, weaker westerlies over the Arabian Sea prevail. Further investigation with velocity potential with divergence field at 200 hPa level is presented in Figure 7a for preceding spring and Figure 7b for succeeding spring. During preceding spring two significant zones of convergence over central and northern equatorial Pacific Ocean are depicted. Over

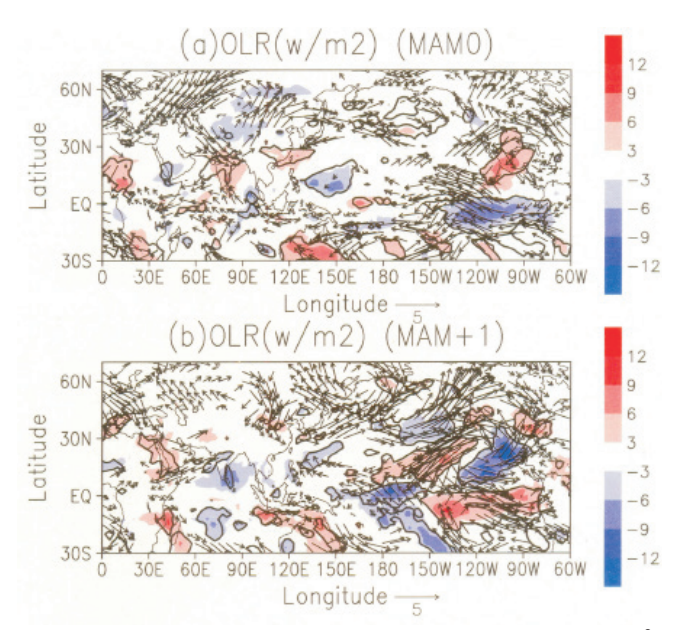


Figure 6: Composite difference of OLR (shaded: W/m²) and 850 hPa wind (vector: m/s) between excess and deficit years during (a) preceding spring and (b) succeeding spring respectively. Black contours represent significant OLR regions at 99% confidence interval. Similarly winds at 99% significant levels are only plotted.

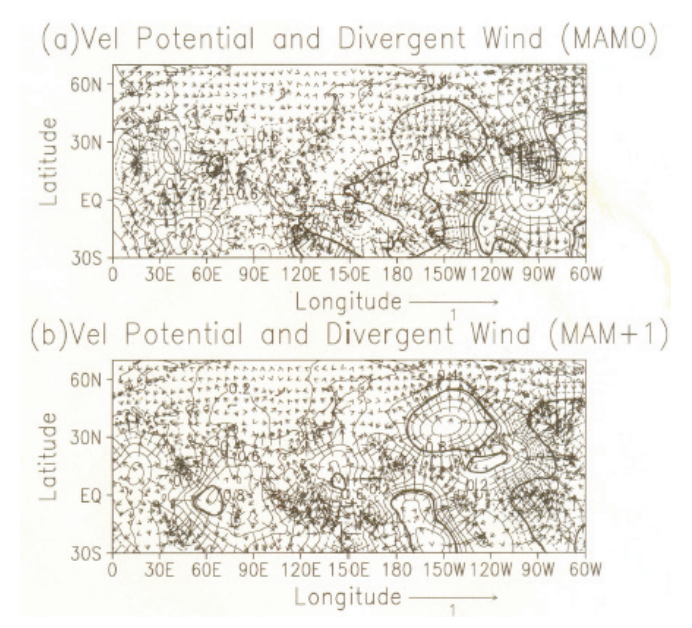


Figure 7: Composite difference of velocity potential with divergence field at 200 hPa level is presented for (a) preceding spring and (b) succeeding spring. Black contours represent significant regions at 99% confidence interval.

Indian subcontinent too, zone of convergence over the Arabian Sea and eastern Indian coast dominate. In case of succeeding spring zone of convergence during preceding spring reverses to the significant zone of divergence, and weaken the convergence over the Indian subcontinent. Additionally, a strong zone of convergence over the Indonesian region exists.

Conclusions

In the present study, association of spring predictability barrier with ISM is studied. Transition during spring (March, April and May) and its implication in following summer monsoon (June, July, August and September) is discussed. Coupling of ISM with preceding and succeeding spring shows critical reversal. During preceding spring strong significant convection dominates over the southern equatorial eastern Pacific Ocean, northern equatorial western Pacific Ocean, Indonesian throughflow and weaker significant convection dominates over the Head Bay of Arabian Sea and western to central Indian subcontinent. Such patterns reverse during succeeding spring. Weaker 850 hPa westerlies over the eastern equatorial Pacific Ocean and Indian Ocean are seen during preceding spring, which during succeeding spring is seen over the Arabian Sea. Further significant zone of divergence during preceding spring reverses to zone of convergence during succeeding spring.

Results related to persistence and transition pertaining to spring and ISM coupled systems shown here are from 1979 to 2008. There could be decadal changes in interannual variability of ENSO/ISM, which needs to be still verified and studied. This particular study will be helpful in providing important input for Indian monsoon research community in view of the policy framing towards agriculture etc.

References

- Ailikun, B. and Yasunari, T., 2001. ENSO and Asian summer monsoon: Persistence and Transitivity in the season March. *J. of the Meteoro. Soc. of Japan*, **79(1):** 145-159.
- Annamalai, H., Hamilton, K. and Sperber, K.R., 2007. South Asian Summer Monsoon and its relationship with ENSO in the IPCC AR4 simulations. *J. Climate*, **20:** 1071-1092.
- Goswami, B.N., Krishnamurthy, V. and Annamalai, H., 1999. A broad-scale circulation index for the interannual variability of the Indian summer monsoon. *Q. J. R. Meteoro. Soc.*, **125:** 611-633.
- Hadley Centre, 2006. HadiSST 1.1 global sea-ice coverage and SST (1870-present). British Atmospheric Data Centre. http://badc.nerc.ac.uk/data/hadisst.

- Indian Institute of Tropical Meteorology (IITM), Pune, India. http://www.tropmet.res.in/Data%20Archival-51-Page
- Kanamitsu, M., Ebisuzaki, W., Woollen, J., Yang, S.-K., Hnilo, J.J., Fiorino, M. and Potter, G.L., 2002. NCEP-DEO AMIP-II reanalysis (R-2). *Bull. Amer. Met. Soc.*, **181:** 2631-2644.
- Karamuri, A., Weng, H., Behera, S., Rao, S.A. and Yamagata, T., 2007. El Niño Modoki and its teleconnection. *J. Geophys. Res.*, 112: C11007, doi:10.1029/2006JC003798.
- Karamuri, A., Tam, C.-Y. and Lee, W.-J., 2009. ENSO Modoki impact on the Southern Hemisphere storm track activity during extended austral winter. *Geophys. Res. Lett.*, 36: L12705, doi:10.1029/2009GL038847.
- Kim, H.-M., Webster, P.J. and Curry, J.A., 2009. Impact of shifting patterns of pacific ocean warming on north Atlantic tropical cyclones. *Science*, **325**: 77-80.
- Koteswaram, P., 1958. The easterly jet stream in the tropics. *Tellus*, **10(1)**: 43-57.
- Kriplani, R.H. and Kulkarni, A.A., 1997. Climatic impact of El Nino and La Nina on the Indian monsoon: A new perspective. *Weather*, **52:** 39-46.
- Krishnakumar, K., Rajagopalan, B. and Cane, M.A., 1999. On the weakening relationship between Indian monsoon and ENSO. *Science*, **284**: 2156-2159.
- Krishnakumar, K., Rajagopalan, B., Hoerling, M., Bates, G. and Cane, M.A., 2006. Unraveling mystery of Indian monsoon failure during El Niño. *Science*, **314**: 115-119.
- Kuchraski, F., Bracco, A., Yoo, J.H. and Molteni, F., 2007. Low-frequency variability of the Indian monsoon-ENSO relationship and the equatorial Atlantic: The "weakening" of the 1980s and 1990s. *J Climate*, **20:** 4255-4265.
- Latif, M. and Graham, N.E., 1991. How much predictive skill is contained in the thermal structure of an OGCM? *TOGA Notes*, **2:** 6-8.
- Liebmann, B. and Smith, C.A., 1996. Description of complete (interpolated) outgoing longwave radiation dataset. *Bull Amer Met Soc*, **77:** 1275-1277.
- Parthsarthy, B., Munot, A. and Kothawale, D., 1995. Monthly and seasonal rainfall series for all India, homogeneous regions and meteorological subdivisions: 1871-1994. Indian Institute of Tropical Meteorology Research Report, No. RR-065.
- Saha, S.K., Haldar, S., Krishnakumar, K. and Goswami, B.N., 2012. Pre-onset land surface processes and 'internal' interannual variabilities of the Indian summer monsoon. *Clim Dyn*, 36: 2077-2089.
- Sontakke, N.A., Pant, G.B. and Singh, N., 1993. Construction of all-India summer monsoon rainfall series for the period: 1844-1991. *J. Climatology*, **6:** 1807-1811.
- Torrence, C. and Webster, P.J., 1998. The annual cycle of persistence in the El-Nino/Southern Oscillation. *Q. J. R. Meteoro. Soc.*, **124:** 1985-2004.
- Turner, A., Sperber, K., Slingo, J., Meehl, G., Mechoso, C.R., Kimoto, M. and Giannini, A., 2011. Modelling Monsoons: Understanding and Predicting Current and Future

Behaviour. *In:* The Global Monsoon System: Research and Forecast, 2nd Edition. World Scientific Series on Asia-Pacific Weather and Climate. C.-P. Chang, Y. Ding, G.N.-C. Lau, R.H. Johnson, B. Wang and T. Yasunari (Eds). World Scientific Publishing Company, Singapore. ISBN: 978-981-4343-40-4).

- Ueno, K. and Aryal, R., 2008. Impact of tropical convective activity on monthly temperature variability during non monsoon season in the Nepal Himalayas. *J Geophys Res*, **113:** D18112, dpo. 10.1029/2007JD009524.
- Wang, B. and Fan, Z., 1999. Choices of south Asian summer monsoon indices. *Bull. Amer. Meteoro. Soc.*, **80:** 629-638.
- Webester, P.J. and Yang, S., 1992. Monsoon and ENSO: Selectively interactive systems. *Q. J. R. Meteoro. Soc.*, **118:** 877-926.
- Wright, P., 1979. Persistence of rainfall anomalies of the central Pacific. *Nature*, **277**: 371-374.

- Wright, P., 1985. The southern oscillation: An ocean atmosphere feedback system? *Bull. Amer. Meteoro. Soc.*, **66:** 398-412.
- Yang, S., Lau, K. and Sankar-Rao, M., 1996. Precursory signals associated with the interannual variability of the Asian summer monsoon. *J. Climate*, **9:** 949-964.
- Yasunari, T., 1990. Impact of Indian monsoon on the coupled atmosphere/ocean systems in the tropical pacific. *Meteoro*. *Atmos. Phys.*, **44:** 29-41.
- Yatagai, A., Kamiguchi, K., Arakawa, O., Hamada, A., Yasutomi, N. and Kitoh, A., 2012. APHRODITE: Constructing a long-term daily gridded precipitation dataset for Asia based on a dense network of rain gauges. *Bull Amer Met Soc*, **93(9):** 1401-1415.
- Yeh, S.W., Kug, J.S., Dewitte, B., Kwon, M.H., Kirtman, B. and Jin, F.-F., 2009. El-Niño in a changing climate. *Nature*, **461**: 511-514.